Two-center interference in high-harmonic generation of H_2^+ in a combination of a mid-infrared laser field and a terahertz field*

Jun Zhang(张军), Xue-Fei Pan(潘雪飞), Tong-Tong Xu(徐彤彤), Hong-Dan Zhang(张宏丹), Hui Du(杜慧), Jing Guo(郭静), and Xue-Shen Liu(刘学深)†

Institute of Atomic and Molecular Physics, Jilin University, Changchun 130012, *China*

(Received 7 June 2016; revised manuscript received 10 October 2016; published online 8 December 2016)

We theoretically investigate the two-center interference in high-order harmonics generated from the H_2^+ in a combination of a mid-infrared laser and a terahertz field by numerically solving the time-dependent Schrödinger equation (TDSE). The interference minima in high-order harmonic generation (HHG) are effectively suppressed when a THz field is added. The contribution to HHG from the two separate nuclei is used to demonstrate the locating order of the harmonic minima. Furthermore, we also investigate the emission time of harmonics. The results show that the intensity of the short path around 60^{th} order after adding a THz field is stronger than that in the mid-infrared laser field, which further illustrates the suppression of the interference minima in HHG.

Keywords: terahertz field, high-order harmonic, two-center interference

PACS: 32.80.Rm, 42.65.Ky, 42.65.Re **DOI:** 10.1088/1674-1056/26/1/013202

1. Introduction

The high-order harmonic generation (HHG) as a highly nonlinear dynamic has been a hot topic, which provides a new way to obtain the extremely short duration attosecond pulse.[1–3] The HHG process can be described as follow: an electron is ionized from the parent core in the laser pulse, then it recollides with the parent core when the laser reverses.[4–6] Molecular high-order-harmonic generation (MHOHG) has attracted much attention due to the application in exploring the complex molecular structure. A special part of MHOHG is the interference phenomena between the contributions from different atomic centers. Lein *et al.*[7] investigated the interference maximum and minima in the harmonic spectra for the two-dimensional H_2^+ molecule within Born–Oppenheimer approximation. They showed that the maximum and the minima depend on the cross angle of the laser polarization and the molecular axis direction, and independent of the laser parameters. The interference phenomenon has been widely investigated,[8–10] where the ionized electron can recollide not only with the parent ion,[4,11] but also with neighboring ions.[12–14] Liu *et al.*[10] investigated the minima based on the Born–Oppenheimer and non-Born–Oppenheimer approximations, respectively. The results show that the positions of the spectral minima are fixed for the Born–Oppenheimer model but change periodically for the non-Born–Oppenheimer one. The molecular above-threshold ionization (MATI) spectra can be used to illustrate molecular interference phenomena, which have been widely investigated theoretically and experimentally.[15,16]

In addition, the investigations on the HHG and the attosecond pulses generation by adding THz fields have attracted the interest of scientists.[17–19] Yuan *et al.*[20] illustrated that the recollision of the electron with the parent ions can be controlled by an intense elliptically polarized laser pulse in a THz field. Ge *et al.*[21] demonstrated that there is an enhancement of the harmonic intensity and a spectral width 33 eV can be obtained after adding a THz field.

The harmonic spectra with moving nuclei and static nuclei were investigated recently for the H_2^+ molecule.[22] The harmonic spectrum becomes smoother and has fewer modulations when the nuclei is moving. It demonstrates that the harmonic emission is sensitive to the nuclear motion. We investigate the interference minimum in HHG through the combination of a mid-infrared laser field and a THz field by numerically solving the non-Born–Oppenheimer time-dependent Schrödinger equation (TDSE). The contribution to HHG from the nucleus along the positive- or negative-z direction is presented, respectively, to further illustrate the interference phenomenon. After we add a THz field, we can see that the harmonic intensity from the nucleus along the positive-z direction is enhanced. The interference minimum can be suppressed and a continuum spectrum can be obtained. The time-frequency analysis is also presented to illustrate the physical phenomenon.

2. Theoretical model

The interference minimum in HHG can be investigated by means of numerical solution of the TDSE of the H_2^+ molecule,

*Project supported by the National Natural Science Foundation of China (Grant Nos. 61575077, 11574117, and 11271158) and the Graduate Innovation Fund of Jilin University, China (Grant No. 2016153).

†Corresponding author. E-mail: liuxs@jlu.edu.cn

© 2017 Chinese Physical Society and IOP Publishing Ltd

the initial wave function is obtained by the finite-element discrete variable representation (DVR) method.[23] The non-Born–Oppenheimer TDSE can be solved by the second-order split-operator approach.[24,25] For the one-dimensional electronic and one-dimensional nuclear model, the z axis is taken to be along the internuclear axis of the diatomic molecules. And it is assumed to be parallel to the polarization direction of the laser pulse. The corresponding TDSE is given as

$$\mathrm{i}\frac{\partial}{\partial t}\Psi(z,R,t) = H(z,R,t)\,\Psi(z,R,t), \tag{1}$$

with

$$H(z,R,t) = T_R + T_z + V_{\mathrm{C}}(z,R) + V_{\mathrm{I}}(z,t), \tag{2}$$

$$T_{\mathrm{R}} = -\frac{1}{m_{\mathrm{p}}}\frac{\partial^2}{\partial R^2}, \tag{3}$$

$$T_z = -\frac{2m_{\mathrm{p}}+m_{\mathrm{e}}}{4m_{\mathrm{p}}m_{\mathrm{e}}}\frac{\partial^2}{\partial z^2}, \tag{4}$$

$$V_{\mathrm{C}}(z,R) = -\frac{1}{\sqrt{(z-R/2)^2+a}} - \frac{1}{\sqrt{(z+R/2)^2+b}} + \frac{1}{R}, \tag{5}$$

$$V_{\mathrm{I}}(z,t) = -\left[1+\frac{m_{\mathrm{e}}}{(2m_{\mathrm{p}}+m_{\mathrm{e}})}\right]zE(t). \tag{6}$$

where R and z are the internuclear distance and the electronic coordinate, respectively; and $m_{\mathrm{e}} = 1$ and $m_{\mathrm{p}} = 1836$ are the electron and the proton masses, respectively. We choose parameters $a = b = 1$ corresponding to the ionization energy -21.1 eV. All the calculations are performed using the attosecond resolution quantum dynamics program LZH-DICP.[26–28]

The laser field in our simulation is defined as $E_0(t) = E_0\exp[-2\ln 2(t^2/\tau_0^2)]\cos(\omega_0 t)$, $E_{\mathrm{THz}}(t) = E_{\mathrm{THz}}\exp[-2\ln 2(t^2/\tau_{\mathrm{THz}}^2)]\cos(\omega_{\mathrm{THz}}t)$. Here, the corresponding laser peak intensities E_0 and E_{THz} are $I_0 = 5\times10^{14}$ W/cm^2 and $I_{\mathrm{THz}} = 1\times10^{13}$ W/cm^2, $\omega_0 = 0.0207$ a.u. corresponds to $\lambda_0 = 2200$ nm, $\omega_{\mathrm{THz}} = 11.3$ THz corresponds to $\lambda_{\mathrm{THz}} = 26400$ nm. The full widths at half maximum (FWHM) τ_0 and τ_{THz} are 7.34 fs and 88 fs, respectively.

The time-dependent electronic probability density can be obtained by

$$P_z(z,t) = \int_0^R \mathrm{d}R|\Psi(z,R,t)|^2. \tag{7}$$

The ionization probability of electron can be obtained by the flux operator method as

$$P(t) = \int_0^t \mathrm{d}t' \int_0^{R_{\mathrm{s}}} \mathrm{d}R\, j(z,R,t'), \tag{8}$$

where

$$j = \frac{1}{\mu_{\mathrm{e}}}\mathrm{Im}\left[\Psi^*\delta(\mathrm{z}-\mathrm{z}_0)\frac{\partial}{\partial \mathrm{z}}\Psi\right], \tag{9}$$

and $\mu_{\mathrm{e}} = \frac{2m_{\mathrm{p}}m_{\mathrm{e}}}{2m_{\mathrm{p}}+m_{\mathrm{e}}}$ is the reduced mass of electron. $z_0 = 25$ a.u. is the flux analysis position for ionization, and $R_{\mathrm{s}} = 25$ a.u. is the absorbing position.[28,29] We set the spatial grid size as 0 a.u.$< R <$ 30 a.u. and -100 a.u.$< z <$ 100 a.u., with the spatial steps $\Delta R = 0.1$ a.u. and $\Delta z = 0.2$ a.u., and the time step of the electron $\Delta t = 0.2$ a.u.

The harmonic spectrum can be obtained by[30,31]

$$a(t) = -\left\langle \Psi(z,R,t)\left|\frac{\mathrm{d}V_{\mathrm{C}}(z,R)}{\mathrm{d}z} + \left(1+\frac{m_{\mathrm{e}}}{2m_{\mathrm{p}}+m_{\mathrm{e}}}\right)E(t)\right|\Psi(z,R,t)\right\rangle, \tag{10}$$

$$P_a(\omega) \sim \left|\frac{1}{T}\int_0^T a(t)\,\mathrm{e}^{-\mathrm{i}\omega t}\,\mathrm{d}t\right|^2. \tag{11}$$

The dipole acceleration distribution in space can be obtained by[13,20]

$$d_{\mathrm{A}}(z,t) = -\int_0^R \Psi^*(z,R,t)\left[\frac{\mathrm{d}V_{\mathrm{C}}(z,R)}{\mathrm{d}z} + \left(1+\frac{m_{\mathrm{e}}}{2m_{\mathrm{p}}+m_{\mathrm{e}}}\right)E(t)\right]\Psi(z,R,t)\,\mathrm{d}R. \tag{12}$$

By using the dipole acceleration distribution, the contribution of each electronic coordinate in HHG can be demonstrated.

3. Result and discussion

We firstly investigate the harmonic spectra with different wavelengths as shown in Fig. 1. The results show that the positions of the minima locate at different harmonic orders. Thus, the minimum depends on the laser parameters in our one-dimensional model of H_2^+ with moving nuclei,[10] which is different from the Born–Oppenheimer approximation case as demonstrated in Ref. [7].

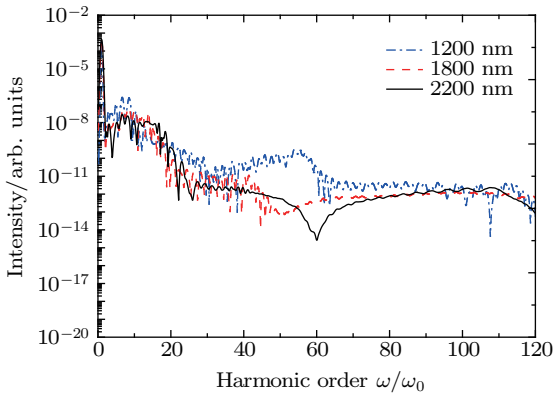


Fig. 1. (color online) High-order harmonic spectrum of H_2^+ driven by few-cycle Gaussian mid-infrared laser pulses with different wavelengths.

Figures 2(a1) and 2(b1) show the electric field (black dashed curve) and the ionization probability (blue solid curve) in a mid-infrared laser pulse and the combination of a mid-infrared laser pulse and a THz field, respectively. The ionization probabilities demonstrate that they begin to increase from

$t = 0$ o.c. which is near the positive peak P_1 (P_1'). The released electron accelerates along the negative-z direction and mainly recombines with the nucleus along the negative-z direction. After that the ionization probabilities begin to increase again around $t = 0.5$ o.c. which is near the negative peak P_2 (P_2'), the ionized electron is accelerated and mainly recombines with the nucleus located in the positive-z axis.

Figures 2(a2) and 2(b2) show the electronic probability densities corresponding to the laser parameters in Figs. 2(a1) and 2(b1), respectively. From Figs. 2(a2) and 2(b2), we can see that the electron is ionized around $t = 0$ o.c. and $t = 0.5$ o.c., which is consistent with the increasing ionization probability in Figs. 2(a1) and 2(b1). Most of the ionized electrons move far from the nuclei, whereas there are still a certain probability on recollision of the electron with the nuclei around 0.5 o.c. and 1.0 o.c. respectively. The probability of the electron recollided with the nucleus around $t = 0.5$ o.c. in the situation of Figs. 2(a2) and 2(b2) is approximately equal. However, the probability of recolliding with the nucleus around 1.0 o.c. with the laser parameters in Fig. 2(a1) is much higher than that in Fig. 2(b1).

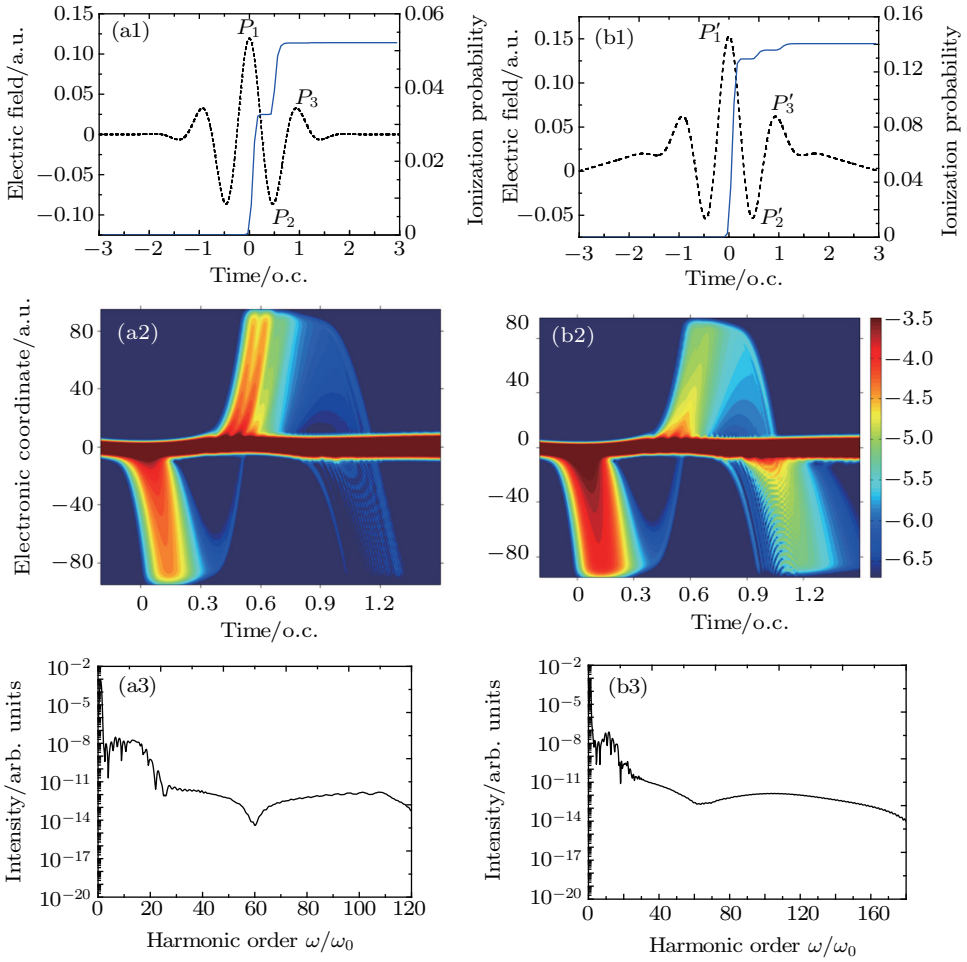


Fig. 2. (color online) Electric field (black dashed curve) and ionization probability (blue solid curve) in (a1) a mid-infrared laser pulse and (b1) the combined laser pulse. Electron probability density distribution in (a2) a mid-infrared laser pulse and (b2) the combined laser pulse. High-order harmonic spectra of H_2^+ in (a3) a mid-infrared laser pulse and (b3) the combined laser pulse.

Figure 2(a3) illustrates the harmonic spectrum corresponding to the laser parameters in Fig. 2(a1). The spectrum clearly presents one minimum in the plateau region around 60^{th} order as demonstrated in Ref. [10]. Figure 2(b3) illustrates the harmonic spectrum corresponding to the laser parameters in Fig. 2(b1), which is extended and forms a smooth plateau from 60^{th} to 180^{th} order. Meanwhile, we can obviously see that the minimum of harmonic emission around 60^{th} order is effectively suppressed.

The harmonic spectral minima originate from the interference between the two atomic centers, which has been illustrated in Ref. [7]. To investigate the effect of two atomic centers, the time-dependent dipole acceleration is divided into two parts as follows: [32]

$$a(t) = a_{z<0}(t) + a_{z>0}(t). \tag{13}$$

In this way, we can demonstrate the HHG spectra of the electron recombined with the nuclei along the positive- or negative-z direction, respectively.

Figures 3(a) and 3(b) show the harmonic spectra obtained

from the dipole acceleration $a_{z<0}(t)$ (solid black curve) and $a_{z>0}(t)$ (dashed red curve), which correspond to the laser parameters in Figs. 2(a1) and 2(b1), respectively.

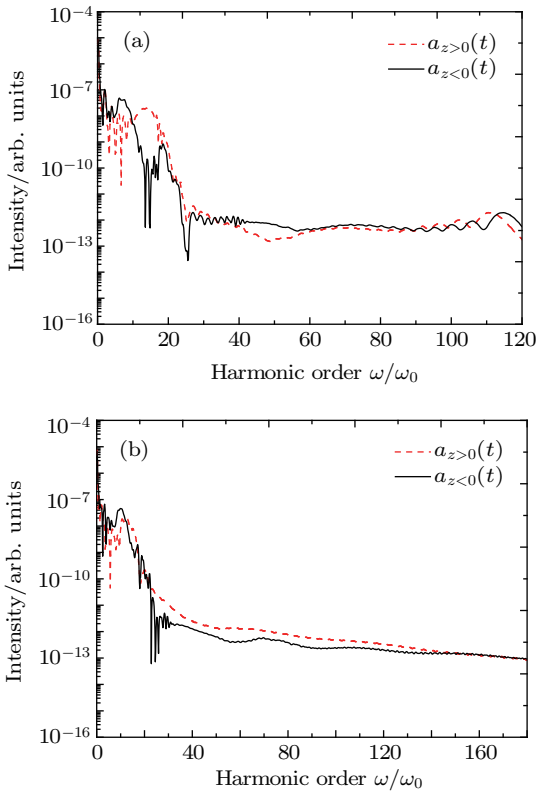


Fig. 3. (color online) Harmonic spectra obtained from the dipole acceleration $a_{z<0}(t)$ (solid black curve) and $a_{z>0}(t)$ (dashed red curve) in (a) the mid-infrared laser pulse and (b) the combined laser pulse.

Figure 3(a) illustrates the harmonic intensity before 34$^{\text{th}}$ order from $a_{z>0}(t)$ is stronger than that from $a_{z<0}(t)$. However, from 34$^{\text{th}}$ to 88$^{\text{th}}$ order, the harmonic intensity from $a_{z<0}(t)$ is a little stronger than that from $a_{z>0}(t)$. The contributions on harmonic emission from the various coordinate has been investigated by the Fourier transform of the dipole acceleration expectation value in Ref. [7]. The sum of these values gives a very small total amplitude, which results in the interference minimum. The HHG spectrum is proportional to the squared modulus of the Fourier transform of the dipole acceleration expectation value. Thus, if the interference minimum appears, the harmonic intensities from $a_{z<0}(t)$ and $a_{z>0}(t)$ are almost equal and the signs of the Fourier transform of the dipole acceleration expectation value are opposite. Otherwise, if the harmonic intensities from $a_{z<0}(t)$ and $a_{z>0}(t)$ are almost equal and the signs of the Fourier transform of the dipole acceleration expectation value are same, or the harmonic intensities from $a_{z<0}(t)$ and $a_{z>0}(t)$ have large difference, the interference minimum will not appear. From Fig. 3(a), we can see that the harmonic intensity around 60$^{\text{th}}$ order from $a_{z<0}(t)$ is almost equal to that from $a_{z>0}(t)$, which is in agreement with the harmonic order of the interference minimum.

Figure 3(b) illustrates that the harmonic intensity from 22$^{\text{nd}}$ to 140$^{\text{th}}$ order from $a_{z>0}(t)$ is stronger than that from $a_{z<0}(t)$, which can be understood from its physical mechanism. When the THz field is added, the laser field peak around $t = 0$ o.c. is increased, which results in a larger probability of the electron ionized along the negative-z axis direction compared to the mid-infrared case shown in Figs. 2(a2) and 2(b2). However, when $t = 0.5$ o.c., the laser field peak is decreased. The ionized electron which is not far away from the nucleus can be driven back to recollide with the nucleus. However, the ionized electron which is far away from the nucleus can not be driven back as demonstrated in Ref. [34] and the recollided probability is almost equal to the case in the mid-infrared laser pulse shown in Figs. 2(a1) and 2(b1). At this time, the contribution to HHG is main from the recombination of the electron with the nucleus along the negative-z direction. After that we also can see that the laser field peak around $t = 1.0$ o.c. is increased. The ionized electron which is far away from the nucleus can also be driven back, which results in a larger recollided probability compared to the case in the mid-infrared laser pulse. At this time, the contribution to HHG is main from the recombination of the electron with the nucleus along the positive-z direction. Meanwhile, we can see that the recollided probability around $t = 1.0$ o.c. is obvious larger than that around $t = 0.5$ o.c. after adding a THz field. Thus, the harmonic intensity from 22$^{\text{nd}}$ to 140$^{\text{th}}$ order from $a_{z>0}(t)$ is stronger than that from $a_{z<0}(t)$ as shown in Fig. 3(b). This obvious harmonic intensity difference indicates that the interference between the two atomic centers has been weakened and results in the suppression of the interference minimum shown in Fig. 2(b3).

We also illustrate the emission time of HHG corresponding to the laser parameters in Figs. 2(a1) and 2(b1), respectively, by using the time-frequency analysis method.[33] Figure 4(a) shows that only one short path makes contribution to the HHG. In the periods of 1.12 o.c. to 1.32 o.c., the short path intensity around 60$^{\text{th}}$ order is much weaker than that of the other orders, which is consistent with the interference minimum of HHG in Fig. 2(a3). Figure 4(b) shows that there is also only one short path making contribution to the HHG. In the periods of 0.75 o.c. to 0.95 o.c., the short path intensity around 60$^{\text{th}}$ order is a little weaker than that of the other orders, which is consistent with the weak minimum of harmonic emission around 60$^{\text{th}}$ order as shown in Fig. 2(b3). Furthermore, from Fig. 2(a1) we can see that the laser field reaches its maximum (0.119 a.u.) around $t = 0$ o.c. When a THz field is added, from Fig. 2(b1) we can see that the laser field reaches its maximum (0.136 a.u.) around $t = 0$ o.c. And the ionization probability is reinforced after adding a THz field. Therefore, in comparison with the mid-infrared laser pulse, the short path intensity is also enhanced after adding a THz field.

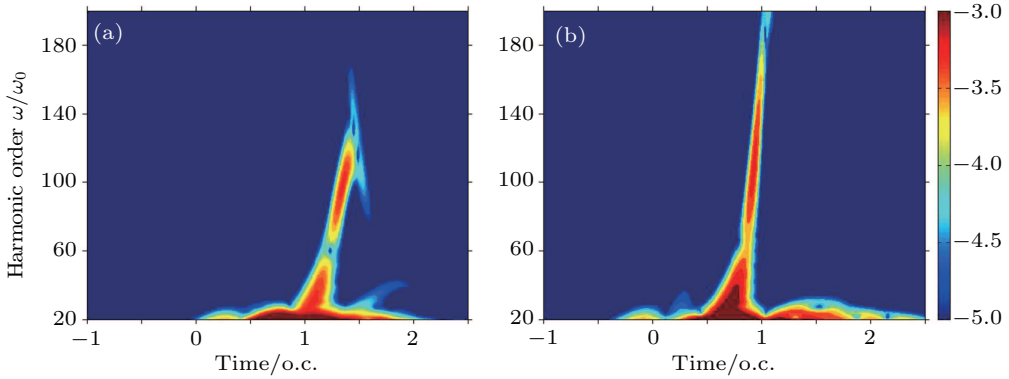


Fig. 4. (color online) Time-frequency distributions of the HHG corresponding to the black solid curves in Figs. 1(a3) and 1(b3), respectively.

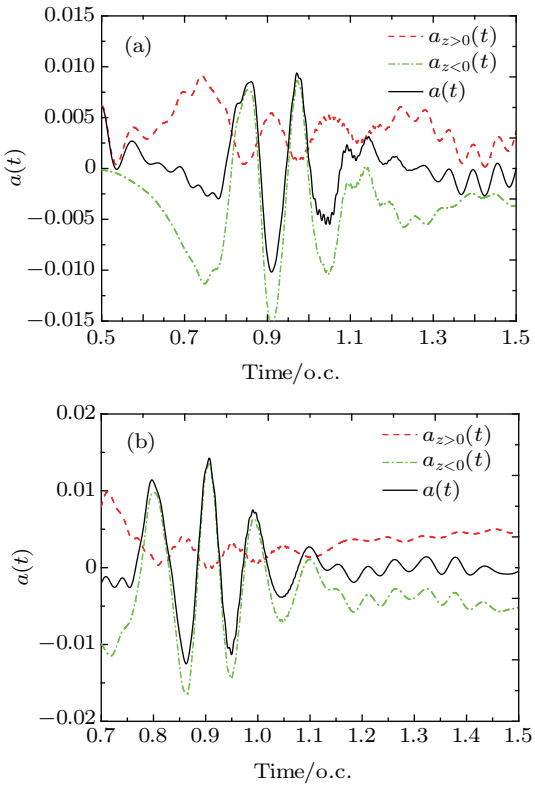


Fig. 5. (color online) The time-dependent dipole acceleration $a_{z<0}(t)$, $a_{z>0}(t)$, and $a(t)$: (a) the mid-infrared laser pulse, (b) the combined laser pulse.

Figures 5(a) and 5(b) illustrate the time-dependent dipole acceleration $a_{z<0}(t)$, $a_{z>0}(t)$, and $a(t)$ corresponding to the laser parameters in Fig. 2(a1) and 2(b1), respectively. Figure 5(a) illustrates that the phases of $a_{z<0}(t)$ and $a_{z>0}(t)$ are opposite in the periods of 1.12 o.c. to 1.32 o.c., which gives negative contributions.[7] And a small total oscillation amplitude of $a(t)$ can be obtained corresponding to the minimum in the plateau region,[9] as presented in Fig. 2(a3). Figure 5(b) illustrates that the overall dipole acceleration amplitude keeps oscillation even in the periods of 0.75 o.c. to 0.95 o.c., which accords with the suppression of the harmonic interference minimum around 60$^{\text{th}}$ order as shown in Fig. 2(b3).

4. Conclusion

We have theoretically investigated two-center interference in the high-order harmonic generation (HHG) of H_2^+ in a combination of a mid-infrared laser field and a THz field. By separating the time-dependent dipole acceleration into two parts along the z axis, we investigate the contribution to HHG from the nucleus along positive- or negative-z direction and demonstrates the locating order of the harmonic minima. When a THz field is added, the contribution to HHG from the nucleus along the positive-z axis direction is enhanced. It results in the suppression of the interference minimum in the HHG and a continuum spectrum can be obtained. The ionization probability and time dependent electron probability density are presented, which illustrate the HHG process as well as the coherent physical mechanism.

Acknowledgments

The authors sincerely thank Prof. Keli Han and Dr. Ruifeng Lu for providing the LZH-DICP code.

References

[1] Kienberger R and Goulielmakis E 2004 *Nature* **427** 817
[2] Corkum P B and Krausz F 2007 *Nat. Phys.* **3** 381
[3] Goulielmakis E and Schultze M 2008 *Science* **320** 1614
[4] Corkum P B 1993 *Phys. Rev. Lett.* **71** 1994
[5] Schafer K J, Yang B, DiMauro L F and Kulander K C 1993 *Phys. Rev. Lett.* **70** 1599
[6] Lewenstein M, Balcou Ph, Ivanov M Yu, L'Huillier A and Corkum P B 1994 *Phys. Rev. A* **49** 2117
[7] Lein M, Hay N, Velotta R, Marangos J P and Knight P L 2002 *Phys. Rev. Lett.* **88** 183903
[8] Qin M, Zhu X, Li Y, Zhang Q, Lan P and Lu P 2014 *Phys. Rev. A* **89** 013410
[9] Cui X, Zhang D Y, Chen G, Chen J G, Zeng S L, Guo F M and Yang Y J 2016 *Chin. Phys. B* **25** 033205
[10] Hu P, Niu Y, Xiang Y, Gong S and Liu C 2015 *Opt. Express* **23** 23834
[11] Bandrauk A D, Chelkowski S and Goudreau S 2005 *J. Mod. Opt.* **52** 411
[12] Bandrauk A D, Chelkowski S, Yu H and Constant E 1997 *Phys. Rev. A* **56** R2537
[13] Bandrauk A D, Barmaki S and Kamta G L 2007 *Phys. Rev. Lett.* **98** 013001

[14] Moreno P, Plaja L and Roso L 1997 *Phys. Rev. A* **55** R1593
[15] Hetzheim H, Figueira de Morisson Faria C and Becker W 2007 *Phys. Rev. A* **76** 023418
[16] Okunishi M and Itaya R 2009 *Phys. Rev. Lett.* **103** 043001
[17] Balogh E and Kovacs K 2011 *Phys. Rev. A* **84** 023806
[18] Du H C, Wang H Q and Hu B T 2011 *Chin. Phys. B* **20** 044207
[19] Kovács K, Balogh E, Hebling J, Toşa V and Varjú K 2012 *Phys. Rev. Lett.* **108** 193903
[20] Yuan K J and Bandrauk A D 2013 *Phys. Rev. Lett.* **110** 023003
[21] Ge X L, Du H, Guo J and Liu X S 2015 *Opt. Express* **23** 8837
[22] Ge X L, Wang T, Guo J and Liu X S 2014 *Phys. Rev. A* **89** 023424
[23] Sharafeddin O and Zhang J Z H 1993 *Chem. Phys. Lett.* **204** 190
[24] Feit M D and Jr J A Fleck 1983 *J. Chem. Phys.* **78** 301
[25] Bandrauk A D and Lu H 2013 *J. Theor. Comput. Chem.* **12** 1340001
[26] Hu J, Han K L and He G Z 2005 *Phys. Rev. Lett.* **95** 123001
[27] Lu R F, He H X, Guo Y H and Han K L 2009 *J. Phys. B* **42** 225601
[28] Lu R F, Zhang P Y and Han K L 2008 *Phys. Rev. E* **77** 066701
[29] Miao X Y and Zhang C P 2014 *Laser Phys. Lett.* **11** 115301
[30] Burnett K, Reed V C, Cooper J and Knight P L 1992 *Phys. Rev. A* **45** 3347
[31] Bian X B and Bandrauk A D 2010 *Phys. Rev. Lett.* **105** 093903
[32] Zhang J, Liu H F, Pan X F, Du H, Guo J and Liu X S 2016 *Chin. Phys. B* **25** 053202
[33] Antoine P, Piraux B and Maquet A 1995 *Phys. Rev. A* **51** R1750
[34] Zhang J, Ge X L, Wang T, Xu T T, Guo J and Liu X S 2015 *Phys. Rev. A* **92** 013418